

Scientific Report

Geological Survey in the Exclusive Economic Zone of the

United States in 2017

(U2017-016)

R/V “Xiangyanghong 10”

10 October 2017– 11 October 2017

Second Institute of Oceanography, Ministry of Natural Resources

16 June 2020

1 Information of the survey

1.1 Survey name

2017 Western Pacific Warm Pool Sediments and Benthos Research Cruise (U2017-016 in the Research Application Tracking System).

1.2 Organization

The organization information is shown in Table 1 as below.

Table 1 The information of the organization

Organization	Second Institute of Oceanography, Ministry of Natural Resources
Address	No.36, Baochubei Road, Hangzhou, Zhejiang, China
Director	Jiabiao Li

1.3 Chief Scientist

The information of the Chief Scientist is shown in Table 2 as below.

Table 2 The information of the Chief Scientist

Name of Chief Scientist	Xu Dong
Country	China
Institute	Second Institute of Oceanography, Ministry of Natural Resources
Address	No.36, Baochubei Road, Hangzhou, Zhejiang, China
Telephone	+86-571-81963167
Email	xudongsio@126.com

1.4 The application and approval situations

There are four designed stations in the exclusive economic zone (EEZ) of the United States for this survey (Fig. 1). The applied survey time in the EEZ of the

United States is from Oct. 10, 2017 to Oct. 20, 2017 (Fig. 2), and the final approved operation time by the US government is also from Oct. 10, 2017 to Oct. 20, 2017 (Fig. 3).

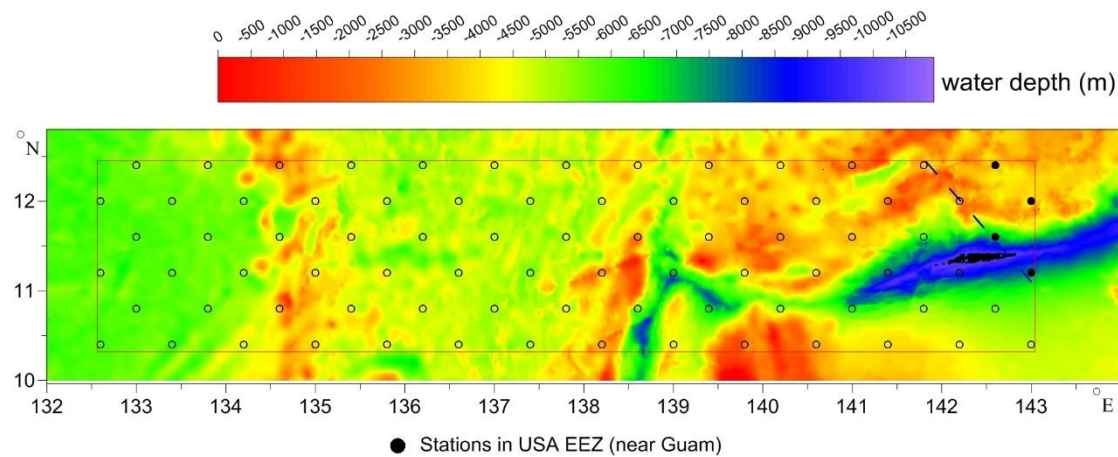


Figure 1 Designed survey stations

4. Coastal States

Coastal State: Guam.

Will you be conducting research in this Coastal State? Yes.

Estimated Entry Date: 10 October, 2017 Estimated Departure Date: 20 October, 2017

Multiple Entries Expected: No

Research will be performed: No less than 94 nm from Guam

Figure 2 The survey time of the application



United States Department of State

Bureau of Oceans and International
Environmental and Scientific Affairs

Washington, D.C. 20520

September 27, 2017

Mr. LIXIN Wang
Embassy of the People's Republic of China
3505 International Place, NW
Washington, DC

Dear Mr. Wang,

I am writing in response to the application to conduct marine scientific research in the Exclusive Economic Zone (EEZ) of the United States of America, listed in the Research Application Tracking System as U2017-016. I am pleased to advise that activities proposed for Xu Dong of the Second Institute of Oceanography, State Oceanic Administration, from October 10, 2017 to October 20, 2017, under U2017-016 are approved, subject to the following conditions being met:

- (1) The marine scientific research is to be undertaken in conformity with the information specified in the research application, and the relevant provisions of U.S. and international law. Plans for any changes in activities, the Chief Scientist or the platform, or the addition of any activities, are to be communicated in advance of entrance into U.S. waters to the Research Coordinator.
- (2) In order to minimize damage to the vent community in the Monument, please utilize the box sampler for collecting rock samples, instead of by trawl.
- (3) The applicant understands that approval of this marine scientific research request does not provide the applicant with exclusive use of the maritime space. At all times, the applicant is to exercise due regard with respect to other lawful uses of the sea. The applicant understands that neither the Department of State nor any other part of the United States Government is responsible for any damage, harm, or liability resulting from the conduct of this marine scientific research by the applicant and that the United States Government assumes no responsibility for any such damage, harm, or liability by virtue of granting this application.
- (4) The applicant will take all steps warranted to apprise mariners of the placement of any potential obstacles to navigation associated with this marine scientific research, including as needed appropriate notifications to the Coast Guard.
- (5) To promote safety by minimizing potential interference with other activities

please contact the CTF74 Battle Watch of positional updates/ changes during transit at the earliest using the following contact information: CSP BWC: 808-473-2517 / and COMPACFLT: 808-471-8625.

- (6) A preliminary report is to be submitted via the Research Application Tracking System no later than thirty (30) days of the end date of this authorization.
- (7) Data from the project will fill gaps in the current coverage of the U.S. extended continental shelf mapping effort and provide baseline maps of areas never before explored. A copy of all data generated during the marine scientific research activities that are the subject of this application are to be sent by email to:
NCEI.Coastal@noaa.gov
Kathryn.Townsend@navy.mil
- (8) A copy of the final report produced that incorporates information obtained from the marine scientific research that is the subject of this application is to be sent to the following addresses:

National Science Foundation
ATTN: B. Houtman
4201 Wilson Boulevard, Suite 725
Arlington, VA 22230

Naval Oceanographic Office
ATTN: Kathryn Townsend
1002 Balch Boulevard
Stennis Space Center, MS 39522-5001

National Centers for Environmental Information
ATTN: Dr. Rost Parsons
NOAA/NCEI
Building 1021, Office 3035
Stennis Space Center, MS 39525

Thank you for your continuing cooperation in these matters.

Sincerely,

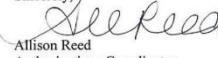

Allison Reed
Authorizations Coordinator
Office of Ocean and Polar Affairs
United States Department of State

Figure 3 The consent letter from the United States

2 Survey completion

The R/V “Xiangyanghong 10” set sail from Zhoushan Port of China on September 1, 2017, entered the EEZ of the United States on October 10, 2017, and left on October 11, 2017 after completing the survey on four stations. “Xiangyanghong 10” finally returned to Zhoushan Port of China on November 4, 2017.

The positions of two applied stations were slightly adjusted, and the notice was sent to the relevant department by email (on October 9, 2017) before entering the EEZ of the United States as required. See Table 3 and Figure 4 for the location of the actual survey stations. See Table 3 for the survey contents of the investigated stations. The surface sediment samples were collected by the box sampler at four stations, and the suspended material (SPM) investigations of the upper 220m water were carried out at station E27 and F26. No trawling or drilling investigations were carried out at these four stations.

Table 3 Actual location and survey contents of the stations in the EEZ of USA

designed location			actual location				survey date	survey contents
No.	latitude (°N)	longitude (°E)	station	latitude (°N)	longitude (°E)	water depth (m)		
1	11.2	143.0	D27	11.729944	143.000442	3960	Oct.10,2017	sediment sampling
2	11.6	142.6	D26	11.730019	142.600006	5020	Oct.10,2017	sediment sampling
3	12.0	143.0	E27	12.000031	143.000000	4200	Oct.11,2017	sediment sampling and CTD operation
4	12.4	142.6	F26	12.407111	142.571975	3560	Oct.11,2017	sediment sampling and CTD operation

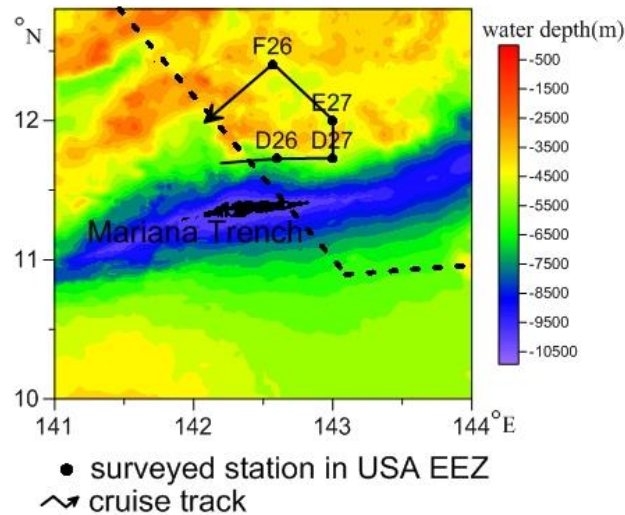


Figure 4 Actual stations and cruise track in the EEZ of the United States

3 Characteristics of surface sediments

3.1 Analysis contents and methods

The sediment type identification and the pH-Eh analysis of sediments from four stations (Figure 5) were conducted in the laboratory of the research vessel. Grain size composition, geochemistry and mineralogy of sediments were analyzed after the cruise.

Because of the rugged seafloor topography and the very thin sediment thickness,

the sediment box samples collected at the four surveyed stations cannot meet the requirements of benthos quantitative analysis, and no large benthos visible to the naked eye were found.

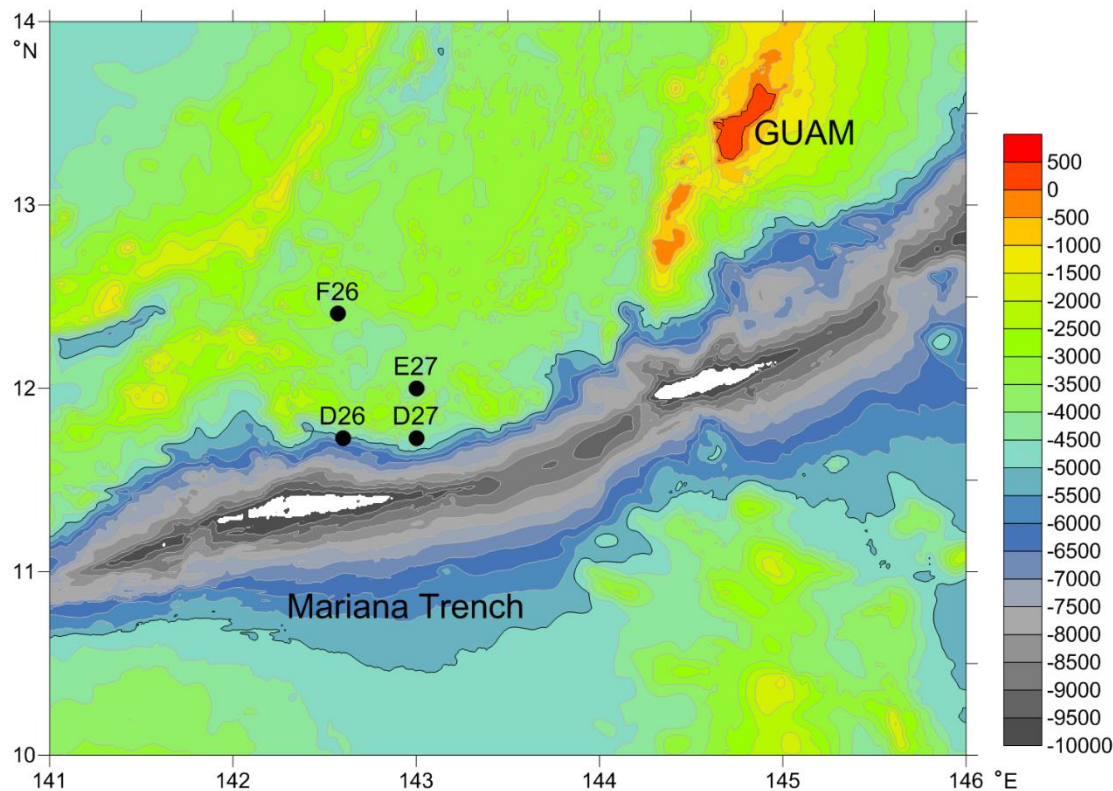


Figure 5 Distribution of survey stations in the EEZ of the United States and seafloor topography nearby

The instrument used for the on-deck pH and Eh analysis of sediments was an acidimeter with an accuracy of 0.01 pH. A pH composite electrode was used for pH test, and an ORP composite electrode was used for Eh test.

The laser particle size analyzer was used for the particle size analysis of sediment samples. Carbonate and organic carbon in samples were completely removed by dilute hydrochloric acid and hydrogen peroxide solutions (30%), respectively. Then, dispersant (sodium hexametaphosphate) was added to the samples. After being processed by the ultrasonic analysis, the samples were analyzed using a Mastersizer 2000 laser analyzer which has a measurement range of 0.02-2000 μm . The grain size parameters, including mean grain size, sorting coefficient, skewness, kurtosis were calculated followed the moment method (McManus, 1988).

The major elements in the sediment were analyzed by X-ray fluorescence

spectrometer (XRF) on fused glass discs samples. The samples wet-digested for trace elements and rare earth elements analysis were analyzed by inductively coupled plasma mass spectrometry (ICP-MS). The contents of carbon and nitrogen in sediments were analyzed by combustion method using an organic element analyzer.

Clay mineral analysis was carried out on the fraction of the sediment with a size of $<2\ \mu\text{m}$, which was separated based on Stokes' settling velocity principle after removal of organic matter and carbonate. XRD analysis were performed on oriented mounts with a diffractometer using $\text{CuK}\alpha$ radiation. Based on the study of the diffraction characteristics of the same sample under different conditions (natural tablet, glycol saturated tablet and heating tablet), the clay minerals were identified. The half quantitative calculation of four main minerals (illite, smectite, chlorite and kaolinite) was carried out on the diffraction pattern of glycol saturated tablet using jade6 software with the empirical factors of Biscaye (1965). The chemical index of illite was estimated using the ratio of the areas of the peaks at $5\ \text{\AA}$ and $10\ \text{\AA}$ in the tablet treated with ethylene glycol. Illite crystallinity was calculated as the full width at half-maximum (FWHM) of the illite peak at $10\ \text{\AA}$.

3.2 Result and Discussion

3.2.1 Surface sediment type

The topography of the investigation region is very complicated. Among the 4 stations surveyed in the EEZ of the United States, three kinds of sediment type were identified by smear, described as follows:

The sediment type of D26 is clay, no calcareous components were found, and the proportion of siliceous component is less than 4%. D26 located at the north slope of Mariana Trench, in the transition zone from seamount to deep trench, with a water depth of 5020m. There were lots of black / gray hard masses, weathered rocks and debris in the sediments (Fig. 6), reflecting the mixed accumulation under the environment of complex seafloor topography. The pH value of the sediment was 7.26, and the Eh value

was 154 mV.



Figure 6 Surface sediment photo of D26

The sediment type of D27 is clayey calcareous ooze. Calcareous component (foraminifera shell) account for about 60%, clay for about 33%, and siliceous component for about 7%. D27 also located in the north slope of Mariana Trench, with water depth only 3960m. There were also many rock debris from nearby seamounts in the sediment (Fig. 7). The pH value of the sediment was 7.64, and Eh value was 170mV, which was slightly higher than that of D26.



Figure7 Surface sediment photo of D27

The sediment type of E27 is diatom ooze. More than 90% of components are fragments of large mat forming diatoms, and nearly no calcareous component or clay were found. E27 located in a lowland surrounded by seamounts (Figure 5), with water depth of 4200m. Mat forming diatoms settling from the upper ocean or sorted after deposition may tend to accumulate in this lowland, forming diatom ooze. According to the research of Zhao et al. (2009) and Xiong et al. (2013), this type of sedimentation is

widely distributed in the Western Pacific Ocean, and the age of diatom ooze concentrated in the Last Glacial Maximum. The pH value of the sediment measured in this station was 7.41, while the Eh value was only 70 mV. The lower Eh value indicating the anoxic sedimentary environment.



Figure 8 Surface sediment photo of E27

The sediment type of F26 station is also clayey calcareous ooze, with about 50% of calcareous components, 41% of clay (mixed with many debris), and 9% of siliceous components. Like E27, F26 also located in lowland surrounded by seamounts with water depth of 3560m. The sediment had dark color (Figure 9), and the pH and Eh values were 7.56 and 78 mV, respectively. The low Eh value also indicating the anoxic sedimentary environment.



Figure 9 Surface sediment photo of F26

We found that the sediment types were closely related to the water depths. On the ridges and seamounts with relatively shallow water depth, the calcareous shells in the sediment were well preserved, and the sediment types were mainly calcareous ooze, calcareous clay and clayey calcareous ooze. While in the basin with water depths of more than 4400m (below CCD), almost all calcareous shells were dissolved, and the sediment types were mainly clay, siliceous clay, siliceous ooze, etc.

3.2.2 Surface sediment grain size characteristics

The sediment type of D26 is clay, and the contents of sand (2-0.063mm), silt (0.063-0.004mm), clay (< 0.004mm) are 27.78%, 50.25% and 21.96%, respectively. The mean grain size of the sediment is 5.76Φ (18 μ m), the median grain size is 17 μ m, and the sorting coefficient is 2.55 Φ . The grain size distribution curve of D26 is wide and gentle, exhibiting generally three peaks (Figure 10), with the characteristics of multi-source mixing.

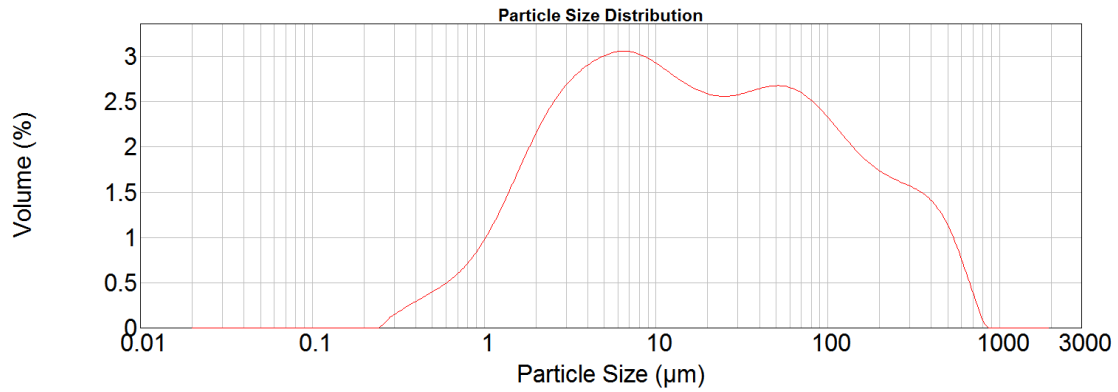


Figure 10 Particle size distribution of D26

For D27, the content of sand, silt and clay are 41.21%, 41.13% and 17.66%, respectively. The mean particle size of the sediment is 4.77 Φ (37 μ m), the median particle size is 38 μ m, and the sorting coefficient is 3.00 Φ , which showing very poor sorting. The particle size distribution curve of D27 also has three obvious peaks and indicating a relatively mixed particle source (Figure 11). The overall particle size of D27 is coarser than that of D26. It should be noted that although the calcareous shells constitute the most important part of the sediment, the carbonate was removed in the pretreatment process, so the particle size distribution mainly reflects the particle size composition of mineral particles and siliceous fragment, in which the coarse-grained rock debris dominates.

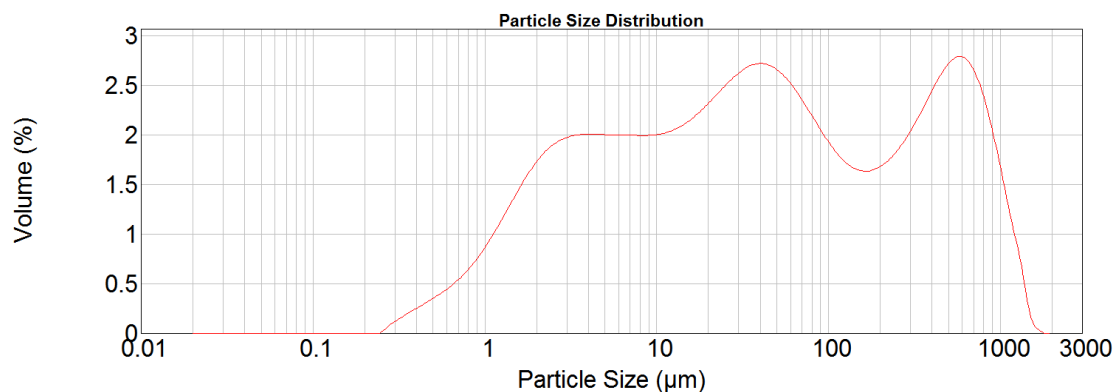


Figure 11 Particle size distribution of D27

For E27, the content of sand, silt and clay is 64.69%, 34.81% and 0.49%, respectively. The mean grain size of sediment is 3.62 Φ (74 μ m), the median grain size is 81 μ m, and the sorting coefficient is 1.14 Φ . There is only one obvious peak in the grain size distribution curve of E27 station (Fig. 12), which indicating a single source

of sediment grains, and that is consistent with the sediment type: diatom ooze.

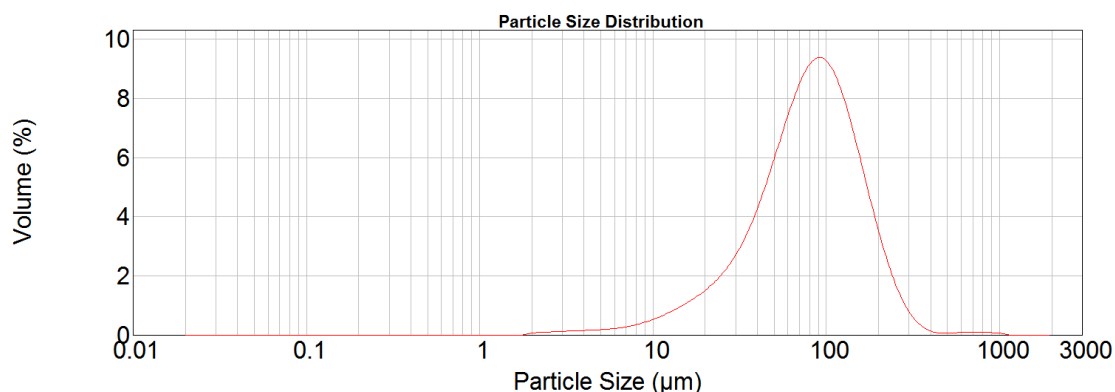


Figure 12 Particle size distribution of E27

Like D27, the sediment type of F26 is clayey calcareous ooze. Carbonate has been removed in the pretreatment, and the result mainly reflects the particle size distribution of mineral particles. The content of sand, silt and clay is 57.00%, 36.85% and 6.15%, respectively. The average particle size of the sediment is 3.67 Φ (57 μ m), the median particle size is 79 μ m, and the sorting coefficient is 2.06 Φ . There is only one obvious peak in the grain size distribution curve of F26 (Fig. 13), and the wide range of fine particles indicates that fine particles are important components.

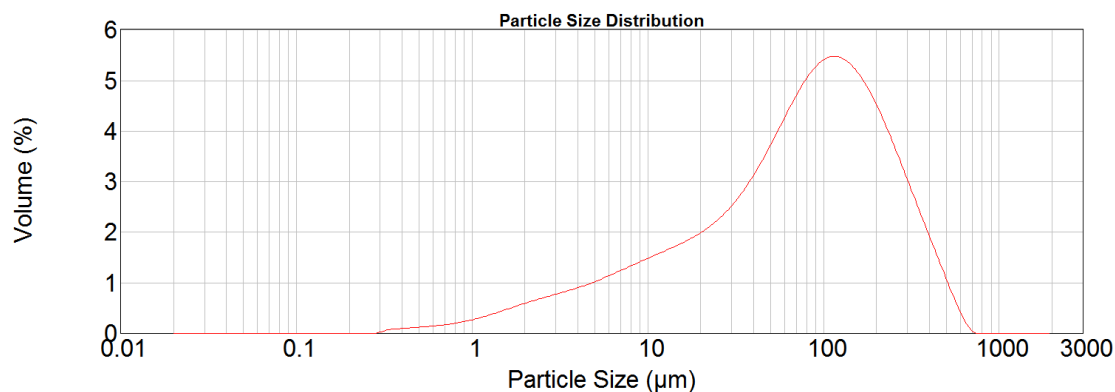


Figure 13 Particle size distribution of F26

3.2.3 Geochemistry of surface sediments

Table 4 shows the statistics of geochemical analysis of the bulk sediments from four stations. The geochemical composition of sediments at each station is quite different due to different sediment types.

Table 4 Statistics of geochemical analysis of surface sediments

component	D26	D27	E27	F26	UCC ^A	surface sediment in East Philippine Sea ^B	core MD06-3047 in West Philippine Sea ^C
SiO ₂ (%)	48.58	32.32	57.38	45.32	65.9	49.16	/
TiO ₂ (%)	0.63	0.36	0.11	0.63	0.5	0.78	0.59
Al ₂ O ₃ (%)	13.19	9.28	2.31	14.20	15.2	15.64	14.06
Fe ₂ O ₃ (%)	9.83	6.05	1.14	6.95	5	9.36	5.99
MnO (%)	1.02	0.23	0.02	0.17	0.08	1.09	0.20
MgO (%)	7.04	4.99	2.11	3.99	2.2	3.58	2.84
CaO (%)	3.79	21.08	1.84	13.31	4.2	2.47	11.75
Na ₂ O (%)	3.86	3.22	11.34	3.77	3.9	4.24	3.37
K ₂ O (%)	1.54	0.94	0.63	0.88	3.4	2.43	1.54
P ₂ O ₅ (%)	0.16	0.12	0.03	0.19	0.15	0.29	0.03
V(10 ⁻⁶)	147.40	118.84	34.90	207.94	107	/	/
Cr(10 ⁻⁶)	364.93	289.93	15.32	59.33	85	/	/
Co(10 ⁻⁶)	82.75	32.75	3.10	22.99	17	/	/
Ni(10 ⁻⁶)	349.67	98.66	6.53	29.53	44	/	/
Cu(10 ⁻⁶)	324.29	98.76	37.84	110.73	25	/	/
Zn(10 ⁻⁶)	144.07	64.70	24.30	63.48	71	/	/
Rb(10 ⁻⁶)	36.03	18.44	8.74	16.61	112	/	/
Sr(10 ⁻⁶)	229.51	581.23	122.20	614.14	350	/	/
Ba(10 ⁻⁶)	301.82	722.69	443.88	566.80	550	/	/
Pb(10 ⁻⁶)	16.85	12.18	2.44	6.66	17	/	/
ΣREE(10 ⁻⁶)	131.78	82.64	25.74	100.06	168.4	/	/
CaCO ₃ (%)	0.38	33.13	0.32	42.28	/	/	/
TOC(%)	0.17	0.28	0.29	0.13	/	/	/
TN(%)	0.08	0.07	0.08	0.07	/	/	/

A: Taylor and McLennan, 1985

B: Xu et al, 2010

C: Xu et al, 2013

As mentioned above, sediment of D26 is mainly composed of mineral debris, with many coarse rock debris. SiO₂, Al₂O₃ and Fe₂O₃ are the components with the highest content. As there is almost no calcareous debris in the sediment, the CaO content is relatively low. The MnO content in the sediment is 1.02%, significantly higher than that in the upper continental crust (UCC) (Fig. 14), we believe that this is because of the exist of micro Fe-Mn nodules, and the growth of Fe-Mn nodules is still at an early stage. The composition of the major elements of D26 is very similar to that of the surface sediments in the East Philippine Sea (Parece Vela Basin) (Xu Zhaokai et al., 2010, table

4). The content of Cr, Co, Ni, Cu, Zn and other metal elements in the sediment of this station is also significantly higher than that of UCC and other three stations (Fig. 15), which may reflect the adsorption effect of Fe-Mn micro nodules on these metal elements.

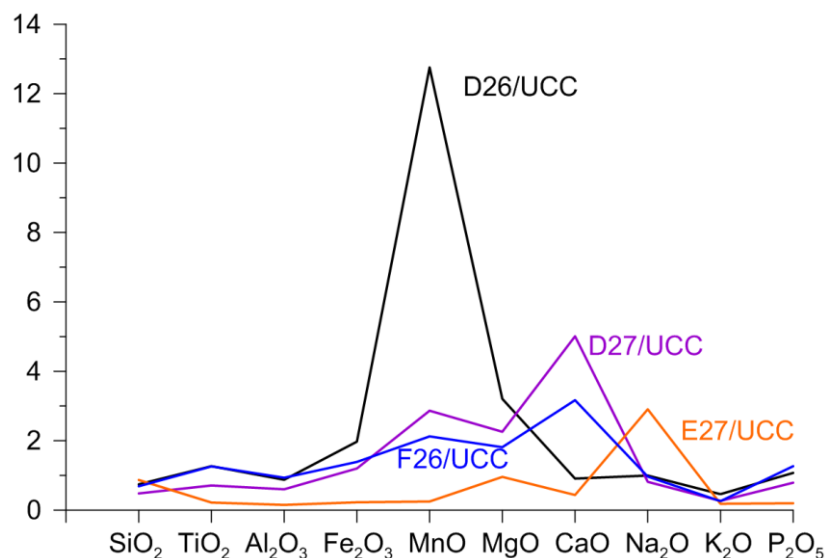


Figure 14 Comparison of the abundance of major elements in sediments with UCC

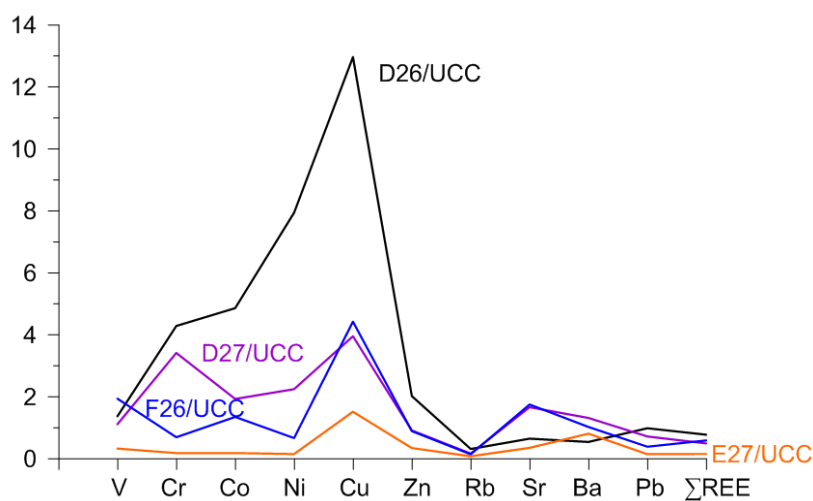


Figure 15 Comparison of the abundance of trace elements in sediments with UCC

The sediment of E27 mainly composed of diatom fragments (Fig. 8), and the SiO₂ content is as high as 57.38%, while the content of other major elements except for Na₂O is at a low level, moreover, the content of most trace elements in the sediment is also much lower than that of UCC and other three stations (Figure 15). The high Na₂O content of 11.34% in E27 may be due to the higher water content of this type of sediment.

There are lot of calcareous shells in sediment of D27 and E26, and the content of CaO is 21.08% and 13.31%, respectively. Accordingly, the SiO₂ content, which is 32.32% and 45.32% respectively, is diluted by CaO. The chemical property of Sr is close to that of Ca, so the content of Sr in the sediment of D27 and E26 is significantly higher than that of the other two stations. Compared with E26, D27 has higher Fe/Al, Mn/Al, and contents of Cr, Co, Ni and other trace elements, indicating that the Fe-Mn micro nodules in D27 should be an important component, which is like in D26.

The rare earth elements (REE) contents in the sediments of four stations are low (Table 5). The \sum REE of E27, which mainly composed of diatom debris, is only 25.74 $\mu\text{g/g}$. The low \sum REE is a major feature of the diatom debris (Xiong et al., 2012). Figure 16 is the REE distribution diagram, and the REE curves of the sediments studied this time are different from that of Chinese loess (Chen et al., 1996) or the core from the East Philippine Sea (Parece Vela Basin) (Ming, 2013). Rare earth elements can be used to trace the source of sediments because of their small fractionation during sediment transport and deposition. We suggest that in addition to the contribution of bioclastic, the main source of the mineral clastic components in the sediments should be the detritus and weathering products of nearby seamounts.

The difference of geographical location and sedimentary environment lead to the difference of sediment type, which is the most important controlling factor of sediment geochemical composition. Station D26 and D27 are both located on the north slope of Mariana Trench, but due to the shallower water depth, D27 contains more calcareous shells, leading to a great difference in geochemical composition from D26. E27 and F26 also located in similar geomorphic environment that surrounded by seamounts, but they have quite different sediment type. E27 have deposited diatom ooze may due to the trapping effect of lowland. As for F26, it may represent the normal sedimentary environment in the back-arc basin surrounded by seamounts.

Table 5 REE composition of surface sediments

REE (10 ⁻⁶)	D26	D27	E27	F26	UCC ^A	Chinese loess ^B	Core PV100609 in East Philippine Sea ^C
La	18.37	10.83	3.65	14.16	30	33	41.04
Ce	31.26	18.48	5.96	25.87	64	59.45	88.99
Pr	4.92	2.89	1.00	3.79	7.1	7.71	10.26
Nd	21.21	12.69	4.24	16.52	26	28.75	41.16
Sm	5.01	3.06	1.01	3.84	4.5	5.5	8.52
Eu	1.35	0.95	0.35	1.25	0.88	1.08	2.08
Gd	5.40	3.37	1.07	3.89	3.8	5.15	8.15
Tb	0.88	0.55	0.17	0.62	0.64	0.77	1.37
Dy	5.23	3.39	1.02	3.63	3.5	4.3	7.79
Ho	1.08	0.71	0.21	0.75	0.8	0.91	1.5
Er	3.08	1.99	0.59	2.13	2.3	2.48	4.13
Tm	0.44	0.29	0.09	0.31	0.33	0.38	0.66
Yb	2.82	1.89	0.53	2.03	2.2	2.42	4.28
Lu	0.43	0.29	0.08	0.30	0.32	0.36	0.71
Y	30.28	21.27	5.78	21.00	22		
ΣREE	131.78	82.64	25.74	100.06	168.4		

A: Taylor and McLennan, 1985

B: Chen et al., 1996

C: Ming, 2013

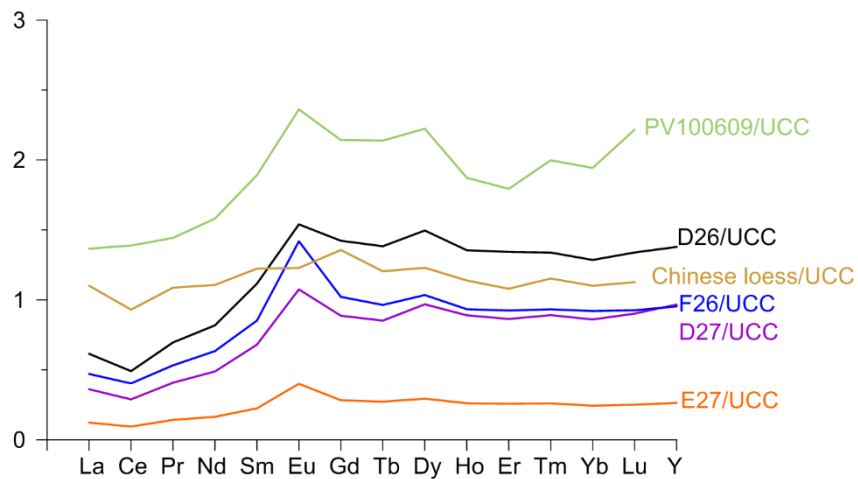


Figure 16 UCC normalized REE patterns of this study and sediments from core PV100609 in East Philippine Sea (Parece Vela Basin) (Ming, 2013), and loess from Chinese Loess Plateau (Chen et al., 1996)

3.2.4 Composition and source of clay minerals

The semi quantitative analysis shows that clay minerals in the sediments are mainly composed of smectite, illite, chlorite and kaolinite (Table 6, Figure 17). D26 and D27 have similar clay mineral composition, showing the illite content ranked first, followed by smectite content, while chlorite and kaolinite are relatively low. E27 and F26 have different clay mineral assemblages compared to D26 and D27, the highest content is smectite, which can be more than 50%, while illite content is the second highest. It is worth noting that the sediment of E27 is mainly composed of diatom fragments, and the amount of clay minerals that extracted from the sediment was very limited, which just barely meet the needs of analysis. So, the result of clay minerals of E27 is only for reference.

Smectite is a widespread clay mineral in ocean sediments. Smectite in marine sediments can be derived from hydrolysis of the rock from the surrounding continent under warm to semi-arid climate conditions (Chamley, 1989), or by halmyrolysis of submarine basic volcanic materials less than a million years old (Chamley, 1989). There is a high content of smectite in the river sediments of Luzon Island, with an average value of 78% (Liu et al., 2009). Luzon Island is the main source of smectite in core MD06-3047 on the Benham Rise of the Western Philippine Basin (Xu et al., 2012). However, the surface current does not support the long-distance transportation of smectite from Luzon and other places to the sea area where shows high smectite content in sediment such as Mariana Trough and the Parece Vela Basin in the East Philippine Sea (Figure 17). Therefore, the smectite in the sediments of these areas mainly come from the weathering of local volcanic materials, such as the Mariana Arc. The smectite in the surface sediments in this study should be derived from the weathering of volcanic materials from the nearby seamounts.

Illite in marine sediment is usually formed from terrigenous clastic rock (Chamley, 1989). It seems that the illite content tends to decrease from north to south from loess in Asia to the Okinawa Trough, Shikoku Basin, eastern West Philippine Sea, Parece Vela Basin and Mariana Trench (Ming et al., 1994). The illite in the core PV090510 in

the Parece Vela Basin is mainly from the Asian continent (Ming et al., 1994). The illite chemical index of each station analyzed in this study is less than 0.3, and the illite crystallinity value is also low (Table 6), which indicates that illite also formed under dry and cold climate with strong physical weathering, and most likely come from the Asian continent transported by East Asian Monsoon.

Typically, detrital mineral chlorite is derived from continental erosion of igneous, metamorphic, or old sedimentary rocks. Kolla et al. (1980) concluded that chlorite had the same distribution pattern as illite in the surface sediment of the whole Philippine Sea, which suggests that chlorite may have the same source as illite. Correlation analysis between clay minerals of core PV090510 also revealed that chlorite has a positive correlation with illite, which indicates chlorite mainly comes from Asian loess by wind (Ming et al., 2014). However, according to Zhang (1994), the chlorite in the Mariana Trough is Fe-Mg chlorite, and the chemical composition of the clays in the Mariana Trough and the West Philippine Basin is obviously different. The chlorite in the Mariana Trough is probably formed by the alteration of mafic volcanic materials in the trough. The chlorite in the four samples in this study may have mixed sources, which should include chlorite from Asian loess and chlorite formed by alteration of mafic volcanic materials nearby.

The warm and humid continental climate is conducive to the formation of kaolinite. The content of kaolinite is generally not high in the Philippine Sea sediments due to the disadvantageous current and transport distance, and it's not surprising that no kaolinite was found in the Mariana Trough sediments (Zhang, 1994). The content of kaolinite of four samples are between 8.3% and 13.3%, which are lower than the content in the sediments near the Philippine Trench (Shi et al., 1995), but significantly higher than that in the Parece Vela Basin (Ming et al., 2014). We suggest that the kaolinite in the investigated area may be mainly imported from Asian aeolian.

Through the analysis of the triangle graph (Figure 17), it can be found that the clay mineral composition of E27 and F26 is relatively similar to that of core MD06-3027 in the West Philippine Sea and core PV090510 in the East Philippine Sea, and the contribution of the weathering products of volcanic materials maybe relatively large.

Instead, D26 and D27 have higher illite and kaolinite content and lower smectite content, and the materials from Asian aeolian have a relatively large contribution to the clay mineral composition.

Table 6 Composition of clay minerals in the sediments of the survey area

station/sediment	smectite (%)	illite (%)	chlorite (%)	kaolinite (%)	illite chemical index	Illite crystallinity ($\Delta 2\theta$)
D26	30.5	40.8	15.4	13.3	0.29	0.34
D27	22.2	53.7	12.2	11.9	0.28	0.27
E27	56.6	26.6	8.5	8.3	0.25	0.27
F26	53.9	23.0	10.5	12.6	0.26	0.27
MD06-3047 ^A	61	23	10	6	/	0.32
PV090510 ^B	46	40	10	4	0.36	0.32
Loess in Lanzhou ^C	3.1	66.7	19.7	10.6	/	/
Loess in Luochuan ^C	13.7	67.3	10	9.5	/	/
Luzon river sediment ^D	77	4	4	16	/	/
DSDP-443 in Shikoku Basin ^E	11	57	25	7	/	/

A: Xu et al., 2012

B: Ming et al., 2014

C: Shi et al., 2005

D: Liu et al., 2009

E: Nagel et al., 1981

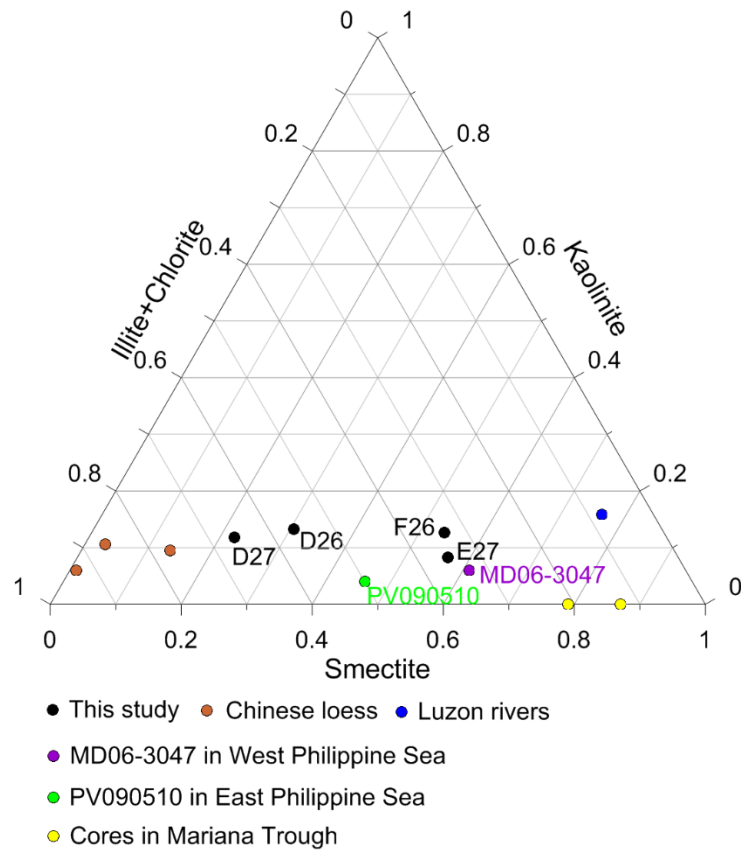


Figure 17 Ternary diagram showing variation in clay minerals compositions of sediments from this study, Luzon rivers (Liu et al., 2009), core MD06-3047 in West Philippine Sea (Xu et al., 2012), core PV090510 in East Philippine Sea (Ming et al., 2014), cores in Mariana Trough (Zhang., 1994), and loess from Chinese Loess Plateau (Shi et al., 2005, Wan et al., 2008)

4 Characteristics of observing factors in upper ocean

4.1 Observing contents and methods

The survey of upper ocean (220m) was carried out at E27 and F26, including the in-situ parameter measurement and the sampling of waters for suspended material concentration analysis.

An SBE 9plus CTD integrated with turbidity and fluorescence chlorophyll sensors was used for the measurement of temperature, salinity, depth, turbidity and chlorophyll concentration.

The in-situ particle size distribution of suspended material in water was measured using a Liss-100x-C laser particle size analyzer, which can detect 32 particle sizes ranging from 2 μ m to 500 μ m. The mean particle size and total volume concentration of suspended material were calculated.

The water samples were collected in 5 layers using a SBE32 water sampler: 1m, 20m, 50m, 100m and 200m. The collected samples were filtered by membrane with bore diameter of 0.45 μ m. The suspended material concentration was calculated according to the ratio of the weight difference before and after filtration to the volume of the filtered water sample.

4.2 Result and Discussion

4.2.1 Suspended material concentration

E27 and F26 are far away from the mainland, and the concentration of suspended material in each layer is very low (Table 7), and the maximum value is only 4.65mg/L. The concentration of suspended material in 100m and 200m layers are slightly higher than that in the upper layers, which may be related to the relative enrichment of plankton in 100m and 200m layers.

Table 7 Results of suspended material concentration at survey stations

station	layer (m)	concentration of suspended material (mg/L)
E27	1	2.41
	20	2.33
	50	2.04
	100	3.00
	200	3.19
F26	1	4.13
	20	3.74
	50	3.83
	100	4.56
	200	4.65

4.2.2 Profiles of observing factors

Fig. 18 and Fig. 19 show the profiles of observing factors in upper ocean of E27 and F26 respectively. The survey stations are in the Western Pacific Warm Pool. The sea surface temperature during this survey was about 30°C, and the water temperature began to decline at about 80m. When the depth reached 220m, the sea water temperature of E27 was about 14.8°C, while that of F26 was about 17.5°C. Although the two stations are not far from each other, the difference of water temperature in thermocline was very significant.

The downward salinity of E27 and F26 began to increase obviously at about 40m, and reached the highest at about 150m. Obviously, the salinity of F26 was slightly higher than E27, and the maximum salinity difference was about 0.15 ‰.

The turbidity of the two stations was very low, with average value less than 0.2 FTU, indicating extremely clear seawater.

Chlorophyll concentration represents the biomass of phytoplankton. It can be seen from Figure 18 and figure 19 that the chlorophyll concentration of both stations was low. The thickness of the maximum zone of chlorophyll content in F26 was larger than E27, and the depth range of the maximum zone of chlorophyll content basically corresponds to the high salinity zone.

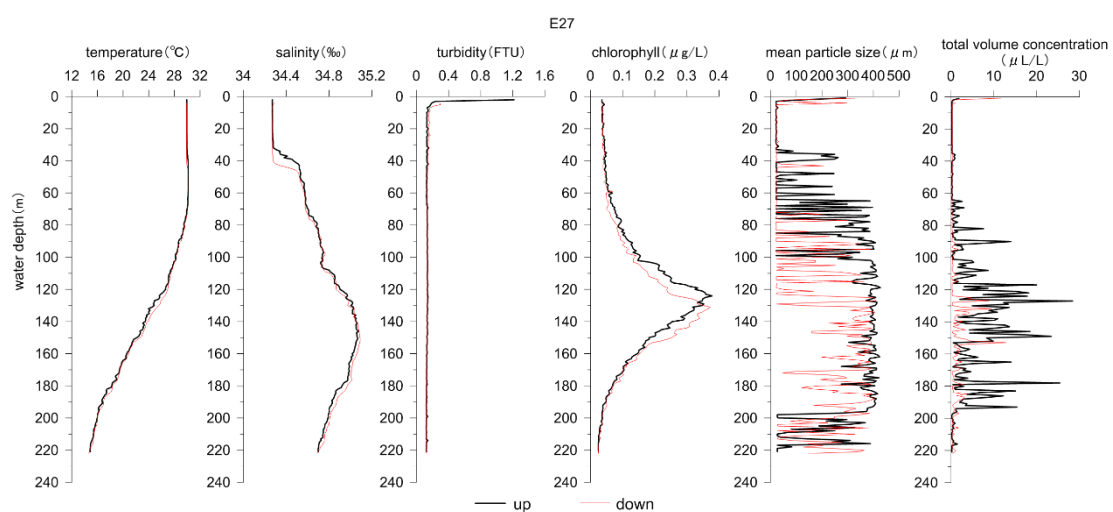


Figure 18 Curves of temperature, salinity, turbidity, chlorophyll, mean particle size and total volume concentration of suspended material of upper water of E27 station

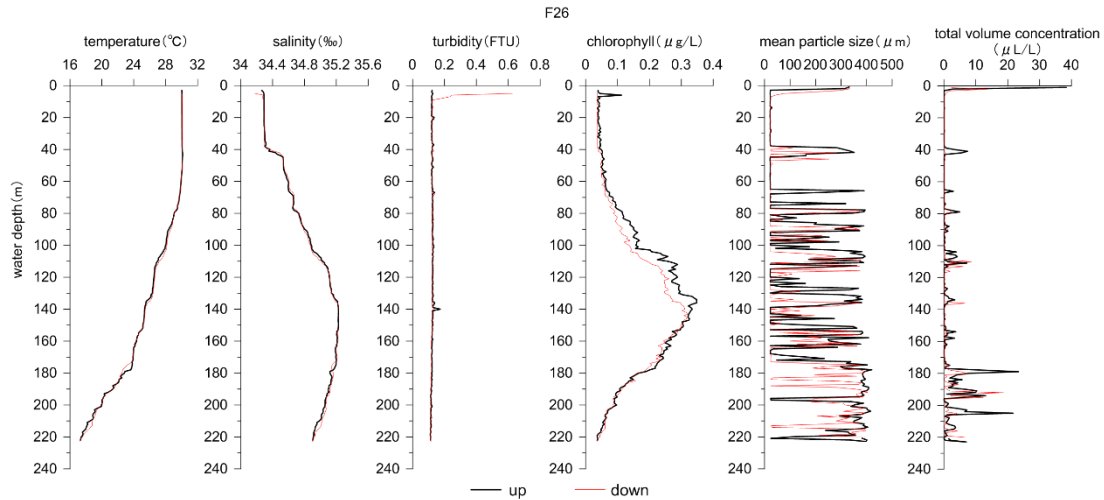


Figure 19 Curves of temperature, salinity, turbidity, chlorophyll, mean particle size and total volume concentration of suspended material of upper water of F26 station

In general, F26 had higher values than E27 in terms of temperature, salinity and the thickness of the maximum chlorophyll content zone.

4.2.2 Mean particle size and total volume concentration of suspended material

From the sea surface to 60m depth, the total volume concentration of suspended particles was at a very low level, and the mean particle size was small, reflecting the scarcity of suspended particles in water (Fig. 18 and Fig. 19). There was a noteworthy phenomenon in E27, that is, in the layer with high chlorophyll content, the total volume concentration and mean particle size of suspended material have increased significantly (Figure 18). In comparison, the total volume concentration of F26 was lower than that of E27, and the high value region of the total volume concentration did not correspond to the maximum value layer of chlorophyll. Moreover, the mean particle size of the suspended material in the maximum chlorophyll layer of F26 was smaller.

The sediment type of E27 is diatom ooze, and the sediment is basically composed of diatom fragments. However, whether there is high concentration of suspended particles mainly composed of diatom in the upper water of E27 is worth further study.

5 Summary

1) There are three types of sediment in the four stations investigated in the EEZ of the United States (near Guam), namely clay (D26), diatom ooze (E27), clayey calcareous ooze (D27 and F26). The sediment types are closely related to water depth and seafloor topography. With the increase of investigation in recent years, it is found that diatom ooze (like in E27) is widely distributed in the Western Pacific, and the low-lying basin topography with multi seamount environment may be conducive to the sorting accumulation of this kind of sediment.

2) The particle size distributions of detrital components after carbonate removal show that D26 and D27 which located on the northern slope of Mariana Trench have smaller mean grain size than E27 and F26 and show the characteristics of multi-source mixing.

3) Sediment type determines the geochemical composition. There are some micro ferromanganese nodules in D26 and D27, and the contents of Cr, Co, Ni, Cu and other metal elements are also significantly higher than those in UCC. The sediment of E27 is mainly composed of diatom fragments, so the Si content is very high, while the content of other elements is very low. The total amount of REE in the four stations are very low, especially in E27.

4) Illite is the dominant clay mineral in the sediments of D26 and D27 which located on the northern slope of Mariana Trench, may reflecting the important contribution of eolian dust from Asia, while smectite is dominant in the other two stations, which may reflect the important contribution of clay minerals formed by weathering of local volcanic materials.

5) E27 and F26 are far away from the mainland, and the concentrations of suspended material in upper water layers are very low, accompanied by low turbidity and chlorophyll concentration, reflecting the lack of suspended material in the upper ocean. F26 had higher values of temperature, salinity and the thickness of the maximum chlorophyll content zone than E27, although the two stations are not far away. However,

the total volume concentration of suspended material in E27 is higher than that in F26.

6) The sediment of E27 is mainly composed of diatom fragments. The questions such as whether there is a high concentration of suspended particles dominated by diatom in the upper water, what's the influence of topography on the productivity of the upper ocean and the selective enrichment of diatom fragments, are worth further study in the future.

6 References

- Biscaye P E. Mineralogy and sedimentation of recent deep sea clay in the Atlantic Ocean and adjacent sea and oceans. *Bulletin of the Geological Society of America*. 1965, 16: 803-832.
- Chamley H. *Clay Sedimentology*. Springer, Berlin. 1989. 623p.
- Chen J, Wang H T, Lu H Y. Behaviours of REE and other trace elements during pedological weathering-evidence from chemical leaching of loess and paleosol from the Luochuan section in central China. *Acta Geologica Sinica*. 1996, 70(1): 61-72. (in Chinese)
- Gingele F X. Holocene climatic optimum in Southwest Africa-evidence from the marine clay mineral record. *Paleogeography, Paleoclimatology, Paleoecology*. 1996, 122(1):77-87.
- Hayward J P, Grenfell H R, Sabea A T, et al. Factors influencing the distribution of Subantarctic deep-sea benthic foraminifera, Campbell and Bounty Plateau, New Zealand. *Micropal*. 2007, 62:141-166.
- Kolla V, Nadler L, Bonatti E. Clay mineral distributions in surface sediments of the Philippine Sea. *Oceanologica Acta*. 1980, 3: 245-250.
- Liu Z F, Zhao Y L, Colin C, Siringan F P, Wu Q. Chemical weathering in Luzon, Philippines from clay mineralogy and major-element geochemistry of river sediments. *Applied Geochemistry*. 2009, 24: 2195-2205.
- McMaus J. Grain size determination and interpretation. In: *Tucker Med. Techniques in*

- Sedimentology. Backwell, Oxford. 1988, 63-85.
- Ming J. The characteristics and provenance of the sediment in the Parece Vela Basin since the Quaternary and their environmental implications. University of Chinese Academy of Sciences. 2013.(in Chinese)
- Ming J, Li A, Huang J, et al. Assemblage characteristics of clay minerals and its implications to evolution of eolian dust input to the Parece Vela Basin since 1.95 Ma. Chinese Journal of Oceanology and Limnology. 2014, 32: 174-186.
- Nagel U, Muller G, Schumann D. Mineralogy of sediments cored during Deep Sea Project Leg 58-60 in the North and South Philippine Sea: results of x-ray diffraction analyses. In : Hussong D M, Uyeda S, Blanchet R et al. eds. Initial Reports of the Deep Sea Drilling Project. 1981. 60 :415-435.
- Shi X F, Chen L R, Li K Y, Wang Z L. Study on minerageny of the clay sediment in the west of Philippine Sea. Marine Geology & Quaternary Geology. 1995, 15: 61-71. (in Chinese)
- Shi Y X, Dai X R, Song Z G, Zhang W G, Wang L Q. Characteristics of clay mineral assemblages and their spatial distribution of Chinese loess in different climatic zones. Acta Sedimentologica Sinica. 2005, 23(4): 690-695. (in Chinese)
- Taylor S R, McLennan S M. The continental crust: its composition and evolution. Melbourne: Blackwell. 1985, 29-45.
- Wan S M, Li A C, Xu K H, Yin X M. Characteristics of clay minerals in the northern South China Sea and its implications for evolution of East Asian Monsoon since Miocene. Earth Science-Journal of China University of Geosciences. 2008, 33(3): 289-300.
- Xiong Z F, Li T G, Algeo T, Chang F M, Yin X B, Xu Z K. Rare earth element geochemistry of laminated diatom mats from tropical West Pacific: evidence for more reducing bottomwaters and higher primary productivity during the Last Glacial Maximum. Chemical Geology. 2012, 296-297: 103-118.
- Xiong Z F, Li T G, Crosta X, et al. Potential role of giant marine diatoms in sequestration of atmospheric CO₂ during the Last Glacial Maximum: $\delta^{13}\text{C}$ evidence from laminated *Ethmodiscus rex* mats in tropical West Pacific. Global and

- Planetary Change. 2013, 108: 1–14.
- Xu Z K, Li A C, Li T G, et al. Major element compositions of surface sediments in the East Philippine Sea and its geological implication. *Mar Geol Quat Geol*. 2010, 30: 43-48. (in Chinese)
- Xu Z K, Li T G, Wan S M, et al. Evolution of East Asian monsoon: Clay mineral evidence in the western Philippine Sea over the past 700 kyr. *Journal of Asian Earth Sciences*. 2012, 60: 188-196.
- Xu Z, Li T, Yu X, Li A, Tang Z, Choi J, Nan Q. Sediment provenance and evolution of the East Asian winter monsoon since 700 ka recorded by major elements in the West Philippine Sea. *Chinese Science Bulletin*. 2013, 58(9): 1044-1052.
- Zhang D Y. Clay mineral composition and distribution in the Mariana Trough. *Journal of Oceanography and Huanghai & Bohai Seas*. 1994, 12(2): 32-39. (in Chinese)
- Zhai B, Li T G, Chang F M, Cao Q Y. Vast laminated diatom mat deposits from the west low-latitude Pacific Ocean in the last glacial period. *Chinese Science Bulletin*. 2009, 54: 4529-4533.

7 Appendixes

- Appendix 1. Station information
- Appendix 2. Sediment type
- Appendix 3. Sediment grain size
- Appendix 4. Sediment pH and Eh
- Appendix 5. Geochemistry
- Appendix 6. Clay mineral
- Appendix 7. SPM concentration
- Appendix 8. SPM size
- Appendix 9. CTD data